

Fig. 5 Velocity versus angular displacement (V8 engine)

attained from the inertia value using the least squares method is consistently smaller than the reference data, and eventually leads to larger velocity estimation error than the average method (Fig. 5).

Some precautions are needed when applying the least squares method to compute the engine inertia value. For engines operating at high speeds, the velocity related term in Eq. (1) could be very large compared with the other terms. This could result in some confusing situations. For instance, engines might decelerate over some portion of the engine operation cycle while the net external torque accelerating the engine is positive; or engines might accelerate while the net external torque is negative. These operation situations might make negative engine inertia value estimations possible, which is not feasible. In other cases, engines might have very small accelerations or decelerations while net external torque is moderate to large. For these cases, the calculation might lead to very large engine inertia values, which is not feasible either. The cases mentioned above are most likely to occur when engines operate at high speeds. Those erroneous data corresponding the situations above must be filtered out before applying the least squares method to the engine inertia value computation.

The criterion used in this study to decide whether data should be used to calculate the engine inertia values is to check the quotient of the net external torque divided by the engine acceleration. This quotient should not be too large or too small relative to the average engine inertia value. Those data whose quotient are significantly away from the average engine inertia value are likely to fall in the situations mentioned above, and those data should not be used in the engine inertia value computation.

## V Conclusions

The engine inertia values calculated by the least squares method guarantees minimum acceleration and velocity estimation errors for engine operating at constant average velocities. As for monotonically accelerating and decelerating engines, simulations in the study show that the engine model with an inertia calculated by the least squares method leads to smaller estimation errors in acceleration but larger estimation errors in velocity than the constant inertia engine model with an average inertia. It is important that the user knows the type of engine, its range of operation, and the type of loading in order to calculate an optimal engine inertia for the control purpose. This study has provided guidance in understanding the effects of engine performance variables and in calculating an appropriate estimate for the engine inertia.

## Acknowledgments

This research has been supported by Ford Motor Company. The authors wish to express their gratitude to Dr. Wayne J. Johnson, and Dr. Davor Hrovat.

## References

- Biezeno, C. B., and Grammel, R., 1954, *Engineering Dynamics*, Vol. 4, Van Nostrand.
- Doughty, S., 1988, "Fundamentals of IC Engine Torsional Vibration," ASME 88-ICE-6, presented at the Energy-Source Technology Conference and Exhibition, New Orleans, LA, Jan. 10-14.
- Shiao, Y., Pan, C-H., and Moskwa, J. J., 1994, "Advanced Dynamic Spark Ignition Engine Modeling for Diagnostics and Control," *International Journal of Vehicle Design*, Vol. 15, No. 6, pp. 578-596.
- Taylor, C. F., 1985, *The Internal-Combustion Engine in Theory and Practice*, Vol. 2, MIT Press.

## Experimental Robustness Study of a Second-Order Sliding Mode Controller

André Blom<sup>1</sup> and Bram de Jager<sup>1,2</sup>

*The design of a Second-Order Sliding Mode Controller is discussed and guidelines are given for tuning. The robustness to unmodeled dynamics and parameter-errors is investigated and tested in an experimental case study. The experimental results, as far as robustness to unmodeled dynamics is concerned, are not better than for a traditional PD-controller. When robustness to parameter-errors is concerned the Second-Order Sliding Mode Controller performs slightly better.*

## Introduction

Mechanical manipulators are controlled to make their end-effector track a desired trajectory. The control is often based on a mathematical model that represents the dynamic behaviour of the system. In practice, this model is never an exact representation of reality. There are always phenomena like unmodeled dynamics, inaccurate parameters and measurement noise that cause model imprecisions. These imprecisions may come from actual uncertainty about the system, or from the deliberate choice for a simplified representation of the system dynamics. The presence of these imprecisions often requires a robust control algorithm.

One class of robust controllers is VSS (Variable Structure System), see Utkin (1977). This class of controllers can be used when the model structure itself is inaccurate, but the inaccuracies are bounded with known bounds. VSS controllers are often used as Sliding Mode Controllers. Characteristic components of Sliding Mode Controllers are sliding hyperplanes  $s(\mathbf{x}, t) = \mathbf{0}$  in the state space.

Recently the traditional sliding control (applying a first-order sliding condition) has been further enhanced, resulting in a 'Second-Order Sliding Mode Control' (SOSMC). The SOSMC was presented by Chang (1990) for MIMO systems in Controllability Canonical Form. Elmali and Olgac (1992) extended the SOSMC-technique to general nonlinear MIMO systems, applying I/O-linearization first.

In this paper the theory of SOSMC in combination with I/O-linearization is tested in an experimental environment to investigate the robustness to unmodeled dynamics (i.e., system

<sup>1</sup> Faculty of Mechanical Engineering, Eindhoven University of Technology, P.O. Box 513, 5600 MB Eindhoven, The Netherlands.

<sup>2</sup> Author to whom all correspondence should be sent.

Contributed by the Dynamic Systems and Control Division of THE AMERICAN SOCIETY OF MECHANICAL ENGINEERS. Manuscript received by the DSCD March 16, 1993. Associate Technical Editor: H. ASADA.

of higher order than the model) and parameter-errors. To tune the SOSMC, a set of guidelines is given to achieve best performance. An expression is given for the tracking accuracy and from this expression we recognize a trade-off between tracking accuracy and damping.

### Preliminaries

Consider a nonlinear system that can be described (exactly) by a MIMO model in 'Controllability Canonical Form,' linear in the control  $\mathbf{u}$  (affine):

$$\dot{\mathbf{x}}^{(n)} = \mathbf{f}(\mathbf{x}) + B(\mathbf{x})\mathbf{u} \quad (1)$$

with

$$\mathbf{x}^{(n)} = [y_1^{(n_1)}, y_2^{(n_2)}, \dots, y_k^{(n_k)}]^T \quad n_1 + n_2 + \dots + n_k = n$$

with

$$\mathbf{x} \in \mathbf{R}^n \quad (\text{state vector})$$

$$\mathbf{u} \in \mathbf{R}^m \quad (\text{input vector})$$

$$\mathbf{y} = [y_1, \dots, y_k]^T \in \mathbf{R}^k \quad (\text{output vector})$$

Superscripts in parenthesis indicate the order of time derivatives.

Under certain conditions, a nonlinear system can be transformed into the 'Controllability Canonical Form' by a technique called I/O-linearization. This technique and the conditions are described by Elmali and Olgac (1992), based on Isidori (1989).

Assume that to control the system a mathematical model of the system is available:

$$\dot{\mathbf{x}}^{(n)} = \hat{\mathbf{f}}(\mathbf{x}) + \hat{B}(\mathbf{x})\mathbf{u} \quad (2)$$

For simplicity we assume that the states can be identified with those of (1). This is not necessary.

Because sliding control requires the uncertainties to be bounded with known bounds, a general assumption is:

$$\mathbf{f}(\mathbf{x}) = \hat{\mathbf{f}}(\mathbf{x}) + \Delta\mathbf{f}(\mathbf{x}) \quad \text{with} \quad \|\Delta\mathbf{f}(\mathbf{x})\| \leq \alpha \quad \forall \mathbf{x} \quad (3)$$

$$B(\mathbf{x}) = \hat{B}(\mathbf{x}) + \Delta B(\mathbf{x}) \quad \text{with} \quad \|\Delta B(\mathbf{x})\| \leq \beta \quad \forall \mathbf{x}$$

In properly controlled systems the state vector  $\mathbf{x}$  will behave bounded, so the uncertainty bounds can be determined.

### MIMO Sliding Control With Second-Order Sliding Condition

A second-order Sliding Mode Control strategy by Chang (1990) defines a zero  $z_0$ , in the "error dynamics":

$$\left(\frac{\partial}{\partial t} + z_0\right)s_i = \prod_{j=1}^{n_i} \left(\frac{\partial}{\partial t} + \lambda_{ji}\right) \int_0^t e_i d\tau \quad (4)$$

$$e_i = y_i - y_{i,d} \quad \text{for} \quad i = 1 \dots k$$

This equation is a set of band-pass filters where the break-frequencies are determined by the selection of the poles ( $\lambda_{ji}$ ) and zero ( $z_0$ ). An integral term in the equation assures zero steady-state errors. Writing (4) in the unfactored (polynomial) form we get (see Chang (1990)):

$$\dot{\mathbf{s}} + Z_0\mathbf{s} = \mathbf{e}^{(n-1)} + C_{n-1}\mathbf{e}^{(n-2)} + \dots + C_1\mathbf{e} + C_0 \int_0^t \mathbf{e} d\tau \quad (5)$$

where  $\dot{\mathbf{s}} = \mathbf{0}$  represents the sliding hyperplanes. Taking time derivatives of (5) yields:

$$\ddot{\mathbf{s}} + Z_0\dot{\mathbf{s}} = \mathbf{e}^{(n)} + \mathbf{e}_p \quad (6)$$

with

$$\mathbf{e}_p = C_{n-1}\mathbf{e}^{(n-1)} + \dots + C_1\dot{\mathbf{e}} + C_0\mathbf{e}$$

and this is used to relate  $\mathbf{s}$  with the control input  $\mathbf{u}$ . The error-vector  $\mathbf{e}_p$  can be computed if all states are measured. Substituting (1) in (6) yields:

$$\ddot{\mathbf{s}} + Z_0\dot{\mathbf{s}} = \mathbf{f} + B\mathbf{u} - \mathbf{x}_d^{(n)} + \mathbf{e}_p \quad (7)$$

Stability is guaranteed if the control is designed as:

$$\mathbf{u} = \hat{B}^{-1}(\hat{\mathbf{u}} - k \cdot \text{sign}(\dot{\mathbf{s}})) \quad (8)$$

$$\hat{\mathbf{u}} = -\hat{\mathbf{f}} + \mathbf{x}_d^{(n)} - \mathbf{e}_p + Z_0\dot{\mathbf{s}} - \Omega\mathbf{s} \quad \text{with} \quad \Omega = \text{diag}(\omega_n^2)$$

and the gain  $k$  is quantified as (see Chang, 1990 and Elmali and Olgac, 1992):

$$k > \frac{\alpha + \beta\|\hat{B}^{-1}\hat{\mathbf{u}}\|}{1 - \beta\|\hat{B}^{-1}\text{sign}(\dot{\mathbf{s}})\|} \quad \text{if} \quad \beta\|\hat{B}^{-1}\text{sign}(\dot{\mathbf{s}})\| < 1 \quad (9)$$

We get the 's-dynamics' by substituting the control (8) in (6):

$$\begin{aligned} \ddot{\mathbf{s}} + k \cdot \text{sign}(\dot{\mathbf{s}}) + \Omega\mathbf{s} + \Delta B\hat{B}^{-1}(k \cdot \text{sign}(\dot{\mathbf{s}}) - Z_0\dot{\mathbf{s}} + \Omega\mathbf{s}) \\ = \Delta\mathbf{f} + \Delta B\hat{B}^{-1}(\mathbf{x}_d^{(n)} - \hat{\mathbf{f}} - \mathbf{e}_p) \end{aligned} \quad (10)$$

As we can see from (8) the control law is discontinuous across  $\dot{\mathbf{s}} = \mathbf{0}$ , which leads to chattering. In general, chattering must be eliminated for the controller to perform properly. This can be achieved by smoothing out the control discontinuity in a boundary layer neighboring the switching surface ( $\dot{\mathbf{s}} = \mathbf{0}$ ). Therefore we don't use the 'signum'-function ( $\text{sign}$ ), but we apply the "saturation"-function ( $\text{sat}$ ) instead for each element  $s_i$  of  $\dot{\mathbf{s}}$ :

$$\text{sat}(s_i, \phi) = \begin{cases} 1 & s_i > \phi \\ \frac{s_i}{\phi} & |s_i| \leq \phi \\ -1 & s_i < -\phi \end{cases} \quad (11)$$

Then, the s-dynamics within the boundary layer become:

$$\begin{aligned} \ddot{\mathbf{s}} + k\Phi^{-1}\dot{\mathbf{s}} + \Omega\mathbf{s} + \Delta B\hat{B}^{-1}(k\Phi^{-1}\dot{\mathbf{s}} - Z_0\dot{\mathbf{s}} + \Omega\mathbf{s}) \\ = \Delta\mathbf{f} + \Delta B\hat{B}^{-1}(\mathbf{x}_d^{(n)} - \hat{\mathbf{f}} - \mathbf{e}_p) \end{aligned} \quad (12)$$

This equation represents a set of second-order low-pass filters.

### Tuning the SOSMC

The lack of tools in nonlinear systems theory now creates a problem; a systematic way of selecting the parameters  $Z_0$ ,  $\omega_n$ ,  $\Phi$ ,  $C_{n-1} \dots C_0$  and  $k$  does not exist. Yet, the influence of the tuning parameters can be evaluated.

First, consider the gain  $k$ . This control parameter is completely determined by the confinements on the uncertainties and can be calculated with (9). For control design purposes, the minimum value of  $k$  is selected, since the least control effort is desired.

Next, we investigate the influence of the zero  $z_0$  in the error-dynamics. Chang (1990) suggested that higher values of the zeros provide more damping in the s-dynamics. As we can see from (10/12),  $z_0$  indeed contributes in the damping of the s-dynamics, but the exact influence is not clear, since the total damping can increase and decrease, depending on the "sign" of the matrix  $\Delta B\hat{B}^{-1}Z_0$ . Simulations, however, indeed show more "damping" when  $z_0$  is increased. This is very likely due to the error-dynamics (4), in whose response  $z_0$  has a 'damping' contribution, recognized as a reduction of the rise-time.

Third, we investigate the influence of  $\omega_n$ . As we can see from the s-dynamics inside the boundary layer (12),  $\omega_n$  sets the break-frequency. Preferably we choose this break-frequency (determining the s-dynamics bandwidth) smaller than the lowest unmodeled structural resonant mode.

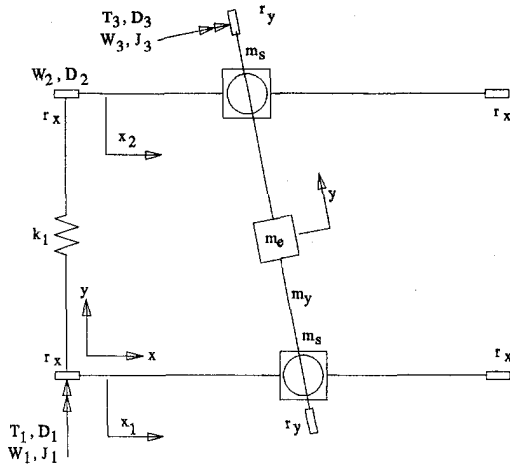


Fig. 1 Schematic representation XY-table

Fourth, to simplify the choice of the poles in the error dynamics (by setting  $C_{n-1} \dots C_0$ ) we can choose the bandwidth of the error dynamics the same as the bandwidth ( $\omega_n$ ) of the s-dynamics. This is not necessary. As we will show, a larger error-dynamics-bandwidth has a positive effect on the tracking error, but may involve a higher control effort.

Fifth, we will motivate the choice of  $\Phi$ , by deriving an expression for the tracking error. Within a finite time  $|\dot{s}| < \Phi$ . Noting that  $\dot{s}$  contains no frequencies higher than  $\omega_n$  (as an approximation) we find:  $|\dot{s}| < \omega_n \Phi$ , so that the maximal tracking error will be (once  $|\dot{s}| < \Phi$  and for the SISO case):

$$|\epsilon| < \frac{\phi(\omega_n + z_0)}{\lambda_1 \lambda_2 \dots \lambda_n} \quad (13)$$

with a guaranteed precision  $\epsilon$  (Blom, 1992).  $\Phi$  has a minimum value, since the implementation has a limited sample frequency. We see from (13) that the zero affects the tracking accuracy in a negative sense also. However, this zero provides damping, which is especially important during transient. We see that there exists a trade-off between tracking accuracy and damping.

## Experiments

To investigate the SOSMC in an experimental environment, the control law was implemented in the control software of an XY-table. In Fig. 1 a schematic top view representation of the XY-table is given. The end effector is a slide with mass  $m_e$ , which can move in the XY-plane by three slideways. Two of them slide in  $x$ -direction and one in  $y$ -direction. The belt wheels of both slideways are driven by servomotors, exerting torques  $T_1$  and  $T_3$ . Coulomb friction appears in all slides and is represented by friction-torques  $W_1$ ,  $W_2$ , and  $W_3$  [Nm]. Viscous damping is represented by  $D_1$ ,  $D_2$ , and  $D_3$  [Nms].

Unfortunately it is not possible to measure the position of the end effector directly. Only three encoder signals are available:  $x_1$ ,  $x_2$ , and  $y$ . We therefore restrict ourselves to the control of motor positions:  $x_1$  and  $y$ .

The belt wheels of the slideways in  $x$ -directions can be connected in two ways:

- (1) With a rigid bar ( $k_1 = \infty$ ), resulting in a (stiff) model with two degrees of freedom:  $x_1$ ,  $y$ , since the translations  $x_1$  and  $x_2$  are equal.
- (2) With a torsion spring with stiffness  $k_1$ , resulting in a (flexible) model with three degrees of freedom:  $x_1$ ,  $x_2$  and  $y$ .

The equations of motion in case of the two degrees of freedom (stiff) model are represented by:

$$\begin{aligned} a_1 \ddot{x}_1 + a_3 \text{sign}(\dot{x}_1) + a_5 \dot{x}_1 &= T_1/r_x \\ a_2 \ddot{y} + a_4 \text{sign}(\dot{y}) + a_6 \dot{y} &= T_3/r_y \end{aligned} \quad (14)$$

with identified parameters:

$$\begin{aligned} a_1 &= J_1/r_x^2 + 2m_s + m_e + m_y = 34 \text{ [kg]} \\ a_2 &= J_3/r_y^2 + m_e = 2.7 \text{ [kg]} \\ a_3 &= (W_1 + W_2)/r_x = 36 \text{ [N]} \\ a_4 &= W_3/r_y = 9 \text{ [N]} \\ a_5 &= (D_1 + D_2)/r_x^2 = 50 \text{ [Ns/m]} \\ a_6 &= D_3/r_y^2 = 8 \text{ [Ns/m]} \\ r_x, r_y &= 0.01 \text{ [m]} \end{aligned}$$

The equations of motion in case of the three degrees of freedom (flexible) model are much more complex and will therefore not be presented.

The desired trajectory to be tracked by the end-effector during all experiments is chosen to be a circle:

$$\begin{aligned} x_d &= 0.5 - r \cos(\omega t) \text{ [m]} \\ y_d &= 0.5 + r \sin(\omega t) \text{ [m]} \end{aligned}$$

with  $r = 0.25$  [m] and  $\omega = \pi$  [rad/s]. The setting of the SMC is tuned up, to get the best results, i.e., the controlled system bandwidth is chosen maximal, with a relative damping in the error dynamics of  $\beta = 0.71$ . The gain  $k$  has been determined by assuming that the available three degrees of freedom model is an exact representation of reality, so that the uncertainty bounds on the two degrees of freedom model can be calculated (3). The control parameters are listed below.

$$\begin{aligned} c_1 &= 63.6 \text{ [rad/s]} \\ c_0 &= 2025 \text{ [rad/s}^2\text{]} \\ \omega_n &= 45 \text{ [rad/s]} \\ z_0 &= 90 \text{ [rad/s]} \\ k &= 70 \text{ [m/s}^2\text{]} \\ \Phi &= 1.11 \text{ [m/s]} \end{aligned}$$

To assess robustness of the SOSMC to unmodeled dynamics, experiments are done with several torsion springs  $k_1$ . The results are compared with a traditional PD-controller, whose setting is also tuned up, resulting in a controlled system break frequency of 45 [rad/s].

To eliminate the trade-off between damping and tracking accuracy, experiments are done while modifying the zero on-line, from the initial (i.e., high) value during transient (damping) to half the initial value (i.e., low) afterward (high tracking accuracy). If switching is only done once, stability is guaranteed. The results for the  $x$ -direction only are shown in Fig. 2. In this figure the tracking error RMS is plotted against the stiffness of torsion spring  $k_1$  (8 springs were available with stiffnesses from 0.19 to 213 [Nm/rad]).

We see that for all stiffnesses  $k_1$  the SOSMC with modification of  $z_0$  realizes a smaller tracking error than an "ordinary" SOSMC, as expected (13). For relatively stiff torsion springs (right side) both SOSMC controllers (with and without modification of  $z_0$ ) realize a smaller tracking error RMS than a PD controller. However, the tracking error RMS for the PD-controller is more constant for a wide range of stiffnesses, in con-

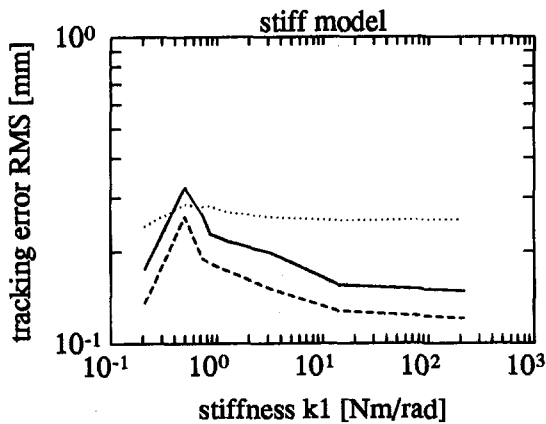


**Fig. 2 Robustness to unmodeled dynamics**  
 solid: SOSMC  
 dashed: SOSMC with modification  $z_0$   
 dotted: PD control

trast with the SOSMC. For one torsion spring ( $k_1 = 0.5$  [Nm/rad]) the tracking error realized with a PD-Controller is even smaller than realized with a SOSMC. We therefore conclude that a PD controller is more robust to unmodeled dynamics (due to stiffness  $k_1$ ) than SOSMC. The level of robustness for both SOSMC is approximately the same.

A strange phenomenon is that for a decreasing stiffness the tracking error RMS increases, but the weakest spring  $k_1$  again yields a small tracking error RMS. This phenomenon can be seen in all experiments and is because we control the motor positions.

To assess robustness to parameter variations, experiments are done with additional mass attached to the end-effector ( $m_e$ ). The results are shown in Fig. 3. In this figure the tracking error RMS is plotted against the additional mass.

For all mass-variations the SOSMC with modification of  $z_0$  realizes the smallest, and the PD-controller the highest tracking error. The tracking error, realized with both SOSMC is more constant for variations in the additional mass, in contrast with the PD-controller. We conclude that both SOSMC are more robust to mass-variations than a PD-controller. Again, the robustness of both SOSMC is approximately the same.

## Conclusions

The main conclusion of this investigation into robustness of the SOSMC is that as far as robustness to unmodeled dynamics

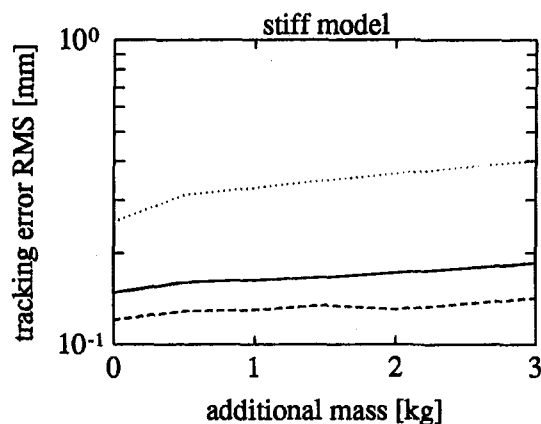


**Fig. 3 Robustness to parameter variations**  
 solid: SOSMC  
 dashed: SOSMC with modification  $z_0$   
 dotted: PD control

is concerned, there is no advantage in using a SOSMC technique in favor of a traditional PD-controller. As far as robustness to parameter errors is concerned, the SOSMC performs slightly better than a PD controller. However, for a large range of operating conditions the SOSMC has far better tracking properties, due to its model based structure, and should be given preference.

## References

- Blom, A., 1993, "Robustness of a Second Order Sliding Mode Controller," Masters thesis, Eindhoven University of Technology, Department of Mechanical Engineering, WFW Report 93.007.
- Chang, L.-W., 1990, "A MIMO Sliding Control with a Second-Order Sliding Condition," ASME WAM, paper no. 90, WA/DSC-5, Dallas, Texas.
- Elmali, H., and Olgac, N., 1992, "Robust Output Tracking Control of Nonlinear MIMO Systems via Sliding Mode Technique," *Automatica*, Vol. 28, No. 1, pp. 145-151.
- Isidori, A., 1989, "Nonlinear Control Systems: An Introduction," Berlin: Springer-Verlag.
- Utkin, V. I., 1977, "Variable Structure Systems with Sliding Modes," *IEEE Transactions on Automatic Control*, Vol. AC-22, Apr., pp. 212-222.

## On Position/Force Control of Robot Interacting With Dynamic Environment in Cartesian Space

Miomir Vukobratović<sup>1</sup> and Radoslav Stojić<sup>1</sup>

*In this paper, the problem of simultaneous stabilization of both the robot motion and interaction force in Cartesian space, based on the unified approach to contact task problem in robotics [1], is considered. This control task is solved under the conditions set on environment dynamics which are less restrictive than those in [1] where some particular environment properties are required to ensure overall system stability. Furthermore, the one-to-one correspondence between closed-loop motion and force dynamic equations is obtained and unique control law ensuring system stability and preset either motion or force transient response is proposed.*

## 1 Introduction

Based on the stability principle of closed-loop control systems the control laws that simultaneously stabilize both the robot motion and interaction force with the environment have been synthesized in refs. [1-5]. These control laws, as distinct from the control laws synthesized using the known traditional approaches [6-10], possess the exponential stability of closed-loop systems and ensure the preset quality of transient responses of motion and interaction force. However, control laws stabilizing desired interaction force with preset quality of transient response are applicable only if the environment possesses "internal stability" property [1]. In this paper, these restrictive conditions are removed and the more general case of dynamic environment is considered. In cases when environment dynamics can be approximated sufficiently well by linear time invariant model in Cartesian space, necessary and sufficient condi-

<sup>1</sup> Robotics Laboratory, Mihailo Pupin Institute, 11000 Beograd, Bosnia.

Contributed by the Dynamic Systems and Control Division of THE AMERICAN SOCIETY OF MECHANICAL ENGINEERS. Manuscript received by the DSCO May 16, 1994; revised manuscript received January 26, 1995. Associate Technical Editor: B. Siciliano.